



HAL
open science

Parahydrophobic and Nanostructured Poly(3,4-ethylenedioxyppyrrrole) and Poly(3,4-propylenedioxyppyrrrole) Films with Hyperbranched Alkyl Chains

Omar Thiam, Alioune Diouf, Samba Yandé Dieng, Frédéric Guittard, Thierry Darmanin

► **To cite this version:**

Omar Thiam, Alioune Diouf, Samba Yandé Dieng, Frédéric Guittard, Thierry Darmanin. Parahydrophobic and Nanostructured Poly(3,4-ethylenedioxyppyrrrole) and Poly(3,4-propylenedioxyppyrrrole) Films with Hyperbranched Alkyl Chains. ACS Omega, 2018, 3, pp.12428 - 12436. 10.1021/acsomega.8b02026 . hal-03554723

HAL Id: hal-03554723

<https://hal.science/hal-03554723>

Submitted on 3 Feb 2022

HAL is a multi-disciplinary open access archive for the deposit and dissemination of scientific research documents, whether they are published or not. The documents may come from teaching and research institutions in France or abroad, or from public or private research centers.

L'archive ouverte pluridisciplinaire **HAL**, est destinée au dépôt et à la diffusion de documents scientifiques de niveau recherche, publiés ou non, émanant des établissements d'enseignement et de recherche français ou étrangers, des laboratoires publics ou privés.

Parahydrophobic and Nanostructured Poly(3,4-ethylenedioxyppyrrrole) and Poly(3,4-propylenedioxyppyrrrole) Films with Hyperbranched Alkyl Chains

Omar Thiam,[†] Alioune Diouf,[†] Samba Yandé Dieng,[†] Frédéric Guittard,^{‡,§} and Thierry Darmanin^{*,‡,§}

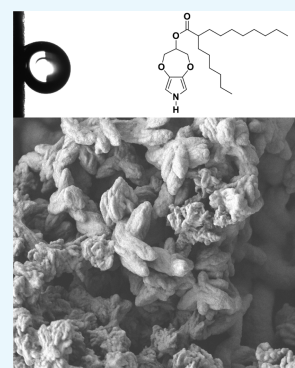
[†]Faculté des Sciences et Techniques, Département de Chimie, Université Cheikh Anta Diop, 5005 Dakar-Fann, Senegal

[‡]NICE Lab, IMREDD, Université Côte d'Azur, 61–63 Av. Simon Veil, 06200 Nice, France

[§]Department of Bioengineering, University California Riverside, Riverside, California 92521, United States

Supporting Information

ABSTRACT: Here, we control the surface hydrophobicity and the adhesion of water droplets by electrodeposition of poly(3,4-ethylenedioxyppyrrrole) (PEDOP) and poly(3,4-propylenedioxyppyrrrole) (PProDOP) with branched alkyl chains placed preferentially on the bridge to favor the formation of nanofibers. Branched alkyl chains of various sizes from very short (C₃) to hyperbranched (C₁₈) are studied because they have lower surface hydrophobicity than long alkyl or fluoroalkyl chains (preferable for parahydrophobic properties). The electrodeposition is much more favored with the PEDOP derivatives because the ProDOP films are more soluble. However, the formation of nanoparticles is favored with the PEDOP polymers in contrast to the formation of fibers, resembling the wax nanoclusters observed on lotus leaves, with the ProDOP polymers. With both these PEDOP and PProDOP derivatives, it is possible to reach parahydrophobic properties characterized by a sticking behavior toward water droplets. This kind of surfaces could be used in the future in water harvesting systems, for example.



1. INTRODUCTION

The need to control surface-wetting properties is very important for various applications, where interfaces are present such as separation membranes, water harvesting apparatus, nonstick pans, anti-icing windows, or antifouling paints.^{1–4} There are numerous examples in nature, where species have special wettability.⁵ For example, the superhydrophobic (both high hydrophobicity and low water adhesion) properties of lotus leaves are a combination of surface structuration at both micro and nanoscale and also the surface energy because the nanoclusters present on these surfaces are composed in a part of hydrophobic waxes.^{6–8} Other species are also capable to attract small water droplets and even fog in hot environments.^{9–12} These properties are known in the literature as parahydrophobic properties, and these surfaces have both high hydrophobicity and high water adhesion. These species include red roses and geckos, for example. For parahydrophobic properties, it is preferable to have surface structuration at only one scale (micro or nano) and also materials of higher surface energy. In particular, one-dimensional (1D) nanostructures such as nanofibers or nanotubes are excellent candidates to control the surface hydrophobicity and water adhesion because these properties are dependent on their length, diameter, orientation to the substrates, and their spacing, for example.^{12–17} Conducting polymers are often used to obtain 1D nanostructures.^{18–20} In the literature, the polyaniline has been extensively studied as a polymer model for the understanding of nanostructure formation, thanks to intra- and intermolecular interactions such as hydrogen bonds and π -

stacking.^{21–25} In particular, Wang et al. used a theoretical model from aniline trimers formed at the beginning of aniline oxidation. This trimer being asymmetric can lead to various assemblies including nanofibers (1D-growth), nanosheets (2D growth), flowerlike or urchinlike structures (3D growth), depending on the experimental conditions (pH, reaction time, etc.).²⁵

For various applications, it is necessary for the growth of nanostructures directly on substrates.¹⁴ In the case of conducting polymers, different processes are possible such as vapor-phase polymerization, plasma polymerization, electropolymerization, or electrografting.^{26,27} Among them, the electropolymerization, also called electrochemical polymerization or conducting polymer electrodeposition, was demonstrated as a fast technique with fine tuning of the surface nanostructures by playing with both electropolymerization parameters (solvent, substrate, concentrations, electrolyte, and deposition method) and the monomer chemical structures.^{28–31} In this process, a monomer is electrochemically oxidized on a working electrode to induce the polymerization and the growth of polymer nanostructures. The electropolymerization is performed on a conductive working electrode not easily oxidizable such as gold, platinum, stainless steel, titania, or transparent indium tin oxide (ITO)-coated glass. For example, aluminum is not a suitable substrate

Received: August 14, 2018

Accepted: September 18, 2018

Published: October 2, 2018

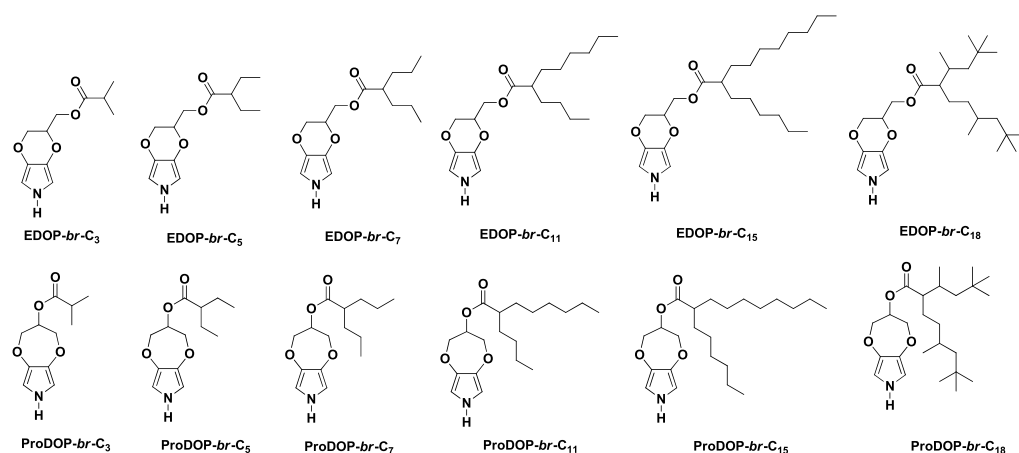


Figure 1. Original monomers studied in this article (EDOP-*br*-R and ProDOP-*br*-R).

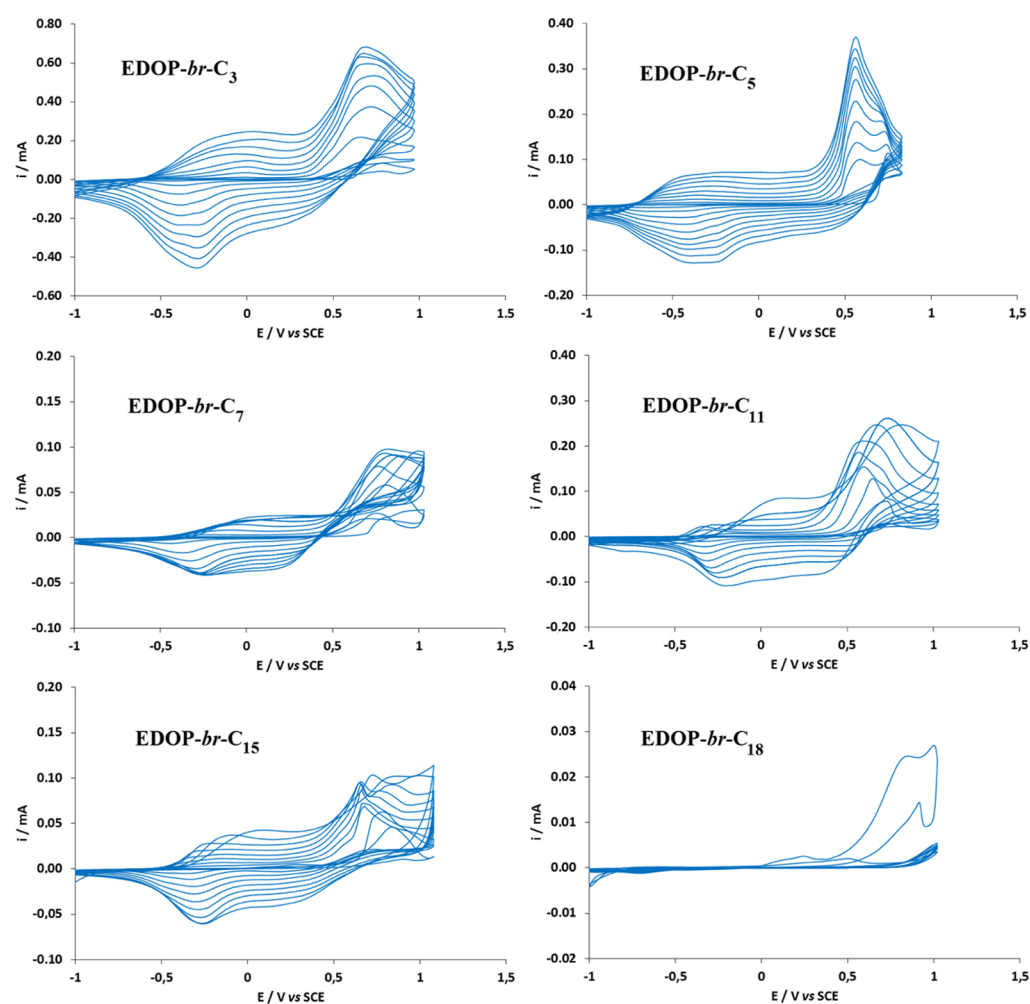


Figure 2. Cyclic voltammograms of the EDOP derivatives (0.01 M) in anhydrous acetonitrile with Bu_4NClO_4 (0.1 M); scan rate: 20 mV s^{-1} .

because of the presence of an oxide layer. The polymer growth can also be controlled with the deposition charge/time or the number of deposition scans. Another advantage is that the process is possible whatever the shape of the substrate such as mesh, textile, foam, or tube. Hydrophobic substituents can also be grafted to change the surface energy even if the substituent can also affect the surface structures. For example, fluorinated and linear alkyl chains were used to obtain superhydrophobic properties, whereas branched alkyl chains and aromatic groups

(substituents of lower hydrophobicity) to obtain parahydrophobic properties.³²

The monomers of the 3,4-alkylenedioxyppyrole family such as 3,4-ethylenedioxyppyrole (EDOP) and 3,4-propylenedioxyppyrole (ProDOP) were now sufficiently studied in the literature.^{33–35} The resulting polymer films are expected to have exceptional optoelectronic properties such as high conductivity, electrochromism, and rapid redox switching.

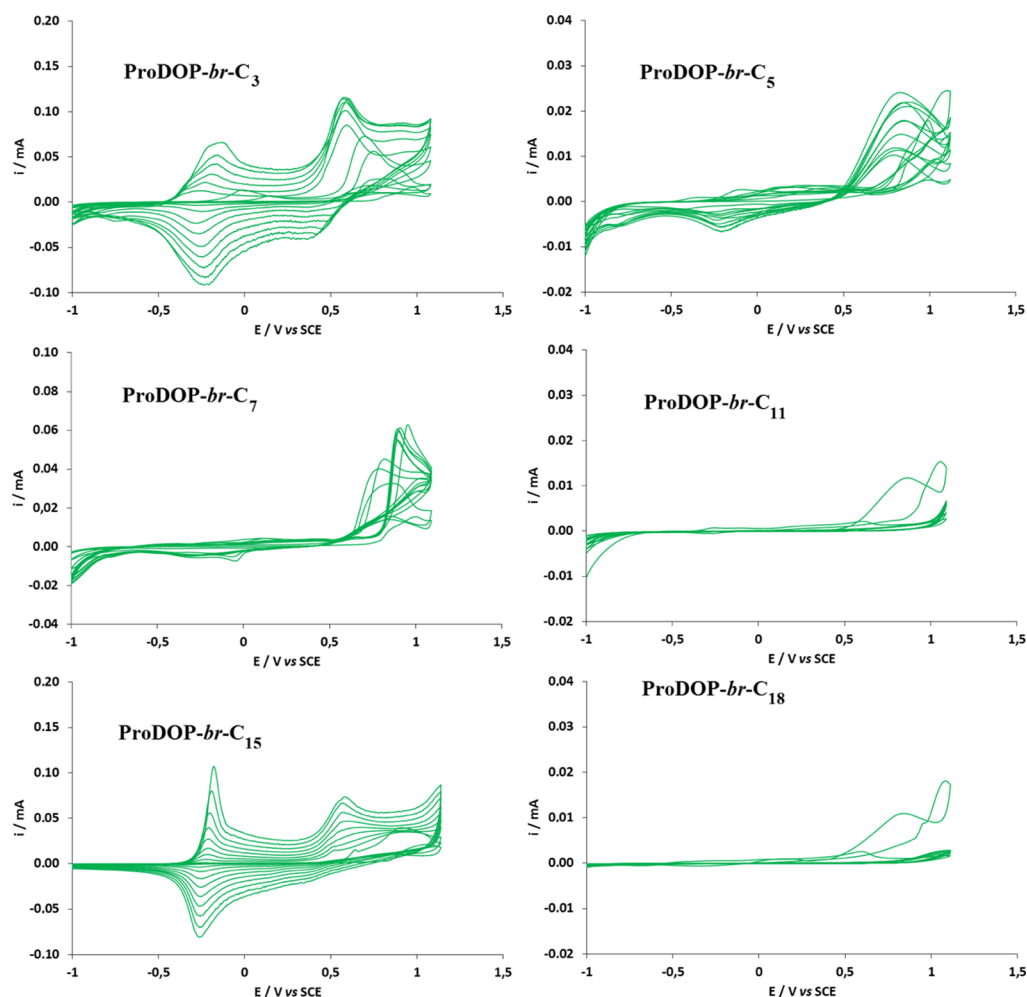


Figure 3. Cyclic voltammograms of the ProDOP derivatives (0.01 M) in anhydrous acetonitrile with Bu_4NClO_4 (0.1 M); scan rate: 20 mV s^{-1} .

For the formation of nanofibers, it is preferable to keep amino (NH) groups free, favoring hydrogen bonds. Indeed, it is possible to place the substituent on the 3,4-ethylenedioxy bridge.^{36,37} Fortunately, it was reported that a very interesting way to synthesize both EDOP and ProDOP derivatives with hydroxyl groups on the bridge is through the reaction with epibromohydrin.³⁸ The formation of nanofibers was found to be possible using fluorinated chains.

Here, to obtain parahydrophobic nanofibers, branched alkyl chains of various sizes from very short (C_3) to hyperbranched (C_{18}) have been grafted on the 3,4-alkylenedioxy bridge of EDOP and ProDOP. Figure 1 shows the different EDOP-*br*-R and ProDOP-*br*-R monomers studied, where different Rs are shown in this figure. The aim is to study their influence on both the formation of nanofibers and the resulting hydrophobic properties. Such materials have potential applications in water harvesting or in water/oil separation.³⁹ In water-harvesting systems, for example, it is important to have as possible both the highest apparent contact angle while having the strongest water adhesion. The aim is to capture water droplets and to release them such that their size becomes higher.

2. RESULTS AND DISCUSSION

2.1. Electrodeposition. First of all, the monomer oxidation potential (E^{ox}) was determined by cyclic voltamme-

try and is between 0.90 and 1.08 V versus saturated calomel electrode (SCE) for the EDOP derivatives and between 1.08 and 1.14 V for the ProDOP derivatives, as a function of the substituent.

Then, cyclic voltammograms were performed to have information of the polymer growth. The cyclic voltammograms are given in Figures 2 and 3. The most significance is the intensity of the peaks, which is much more important using the EDOP monomers, indicating especially higher polymer insolubility and as a consequent a higher amount of polymer on the working electrode (confirmed later in the article). However, the oxidation potentials of the polymers are very low (below 0 V vs SCE), which shows that the polymer chain lengths are long.

To better characterize our polymers, we performed UV–vis absorption spectra. For that, the polymers were electro-deposited on 2 cm^2 ITO substrates but at a constant potential ($E = E^{\text{ox}}$) because it is a better polymerization method for these monomers. A deposition charge of 200 mC cm^{-2} was selected for this characterization. Only the EDOP series was chosen because it was not possible to obtain polymer films with all of the ProDOP monomers. For the UV–vis measurement, it was also necessary to dedope the polymers (for 15 min at -1 V vs SCE) before measurement. The spectra are given in Figure 4. This figure shows that the maximum absorption wavelength (λ_{max}) is approximately the same $\lambda_{\text{max}} \approx$

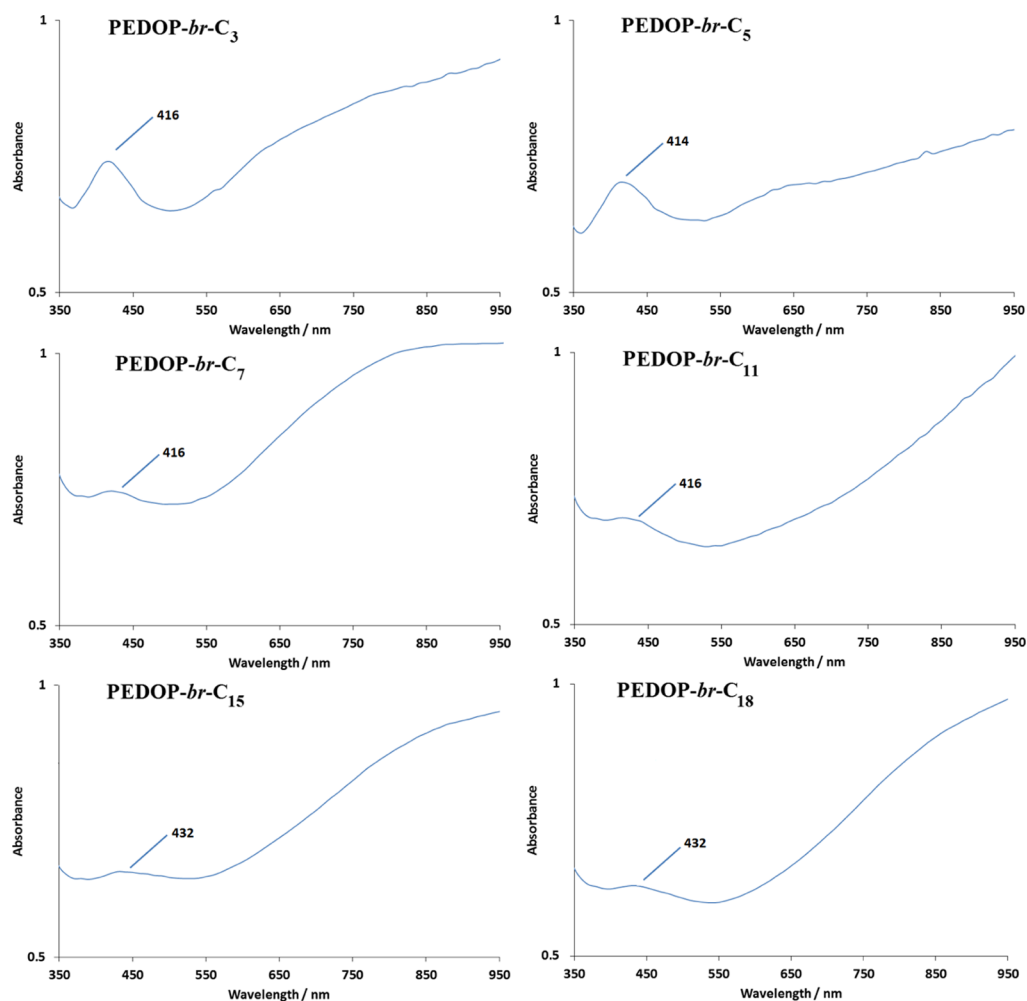


Figure 4. UV-vis absorption spectra of the dedoped PEDOP polymers.

414–416 nm for the polymers with branched alkyl chain from C₃ to C₁₁, whereas it increases a little to ≈432 nm for the longest branched alkyl chains (C₁₅ and C₁₈), which may indicate longer polymer chains. Moreover, all of the spectra display also strong absorption in the long wavelength region, which indicates that these polymers were still in the heavily doped state. This is not surprising because it is known that the polymers of the poly(3,4-alkylenedioxythiophene) and poly(3,4-alkylenedioxyppyrrrole) are extremely stable in their doped state, and as a consequence, it is extremely difficult to fully reduce them.^{33–35}

For the surface characterization, the polymers were electro-deposited on 2 cm² gold plates at a constant potential ($E = E^{ox}$) but using different deposition charges (Q_s from 12.5 to 400 mC cm⁻²) to control the polymer growth.

With the ProDOP monomers, the deposition was possible only with ultralong branched alkyl chains (ProDOP-*br*-C₁₅ and ProDOP-*br*-C₁₈). Hence, the high hydrophobicity of these long branched alkyl chains facilitates their deposition even if they induce important steric hindrance. Hence, using ProDOP-*br*-C₃, even if a peak was present in the cyclic voltammetry curve, the polymer is soluble and cannot form insoluble film on the working electrode. By contrast, using ProDOP-*br*-C₁₈, a thin film is formed but is less soluble.

With the EDOP derivatives, all of the polymers could be deposited because of the higher polymer insolubility, as

observed by cyclic voltammetry. To better understand their solubility, solubility tests in acetonitrile were performed (Table 1). It was observed that all of the PEDOP polymers are more

Table 1. Polymer Solubility in Acetonitrile

polymer	solubility
PEDOP- <i>br</i> -C3	slightly soluble
PEDOP- <i>br</i> -C5	slightly soluble
PEDOP- <i>br</i> -C7	slightly soluble
PEDOP- <i>br</i> -C11	highly insoluble
PEDOP- <i>br</i> -C15	highly insoluble
PEDOP- <i>br</i> -C18	highly insoluble
PProDOP- <i>br</i> -C3	highly soluble
PProDOP- <i>br</i> -C5	highly soluble
PProDOP- <i>br</i> -C7	highly soluble
PProDOP- <i>br</i> -C11	highly soluble
PProDOP- <i>br</i> -C15	soluble
PProDOP- <i>br</i> -C18	soluble

insoluble than the PProDOP polymers whatever the branched alkyl chain. By contrast, the increase in the branched alkyl chain increases the polymer insolubility.

Scanning electron microscopy (SEM) images are given in Figures 5 and 6. For the EDOP derivatives, a very significant change was observed in the surface morphology from smooth to spherical nanoparticles because the branched alkyl chain

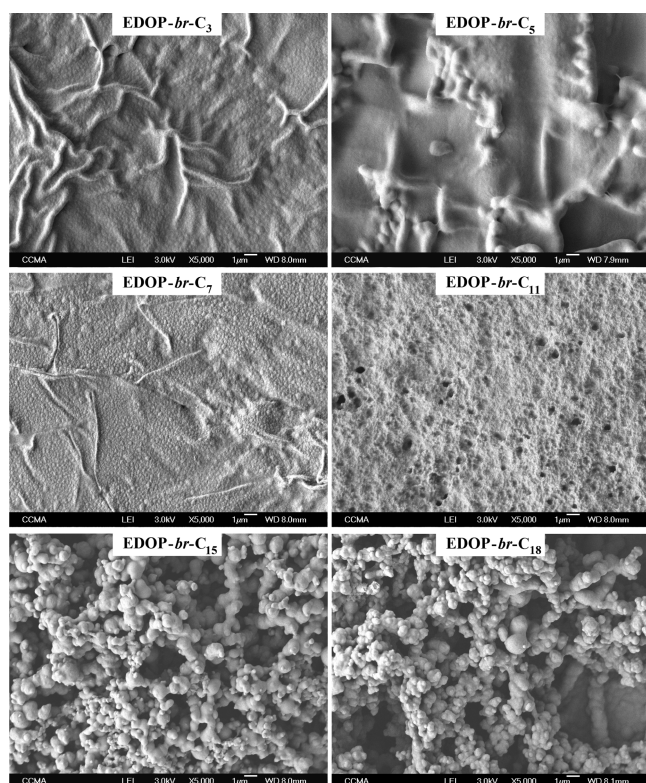


Figure 5. SEM images of the polymer films obtained with the PEDOP derivatives with a deposition charge of 400 mC cm^{-2} .

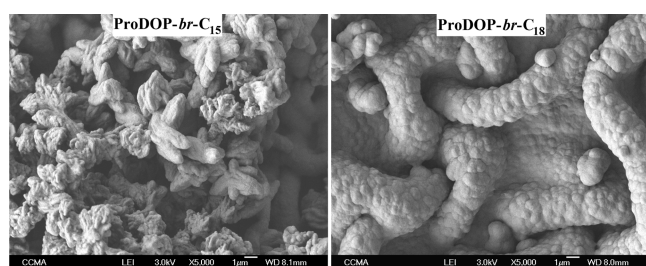


Figure 6. SEM images of the polymer films obtained with the PEDOP derivatives with a deposition charge of 400 mC cm^{-2} .

increases (Figure 5). Moreover, this change is observed from C_{15} branched alkyl chain. This change in the surface morphology confirms previous works showing that it is possible to change the surface morphology from smooth to rough, if there is a huge change in the polymer solubility.⁴⁰ Compared to previous works,³⁷ it should also be noticed that when linear alkyl chains are used, this change takes place with a shorter chain, and even shorter using fluorinated chains showing that the main parameter is the substituent hydrophobicity.

Here, the presence of nanoparticles induces a high increase in the surface hydrophobicity with θ_w up to 135° for $Q_s = 400 \text{ mC cm}^{-2}$ (Table 2). Moreover, these surfaces are completely sticky (parahydrophobic),¹¹ as shown in Figure 7. Water droplets placed on these surfaces remained completely stuck on them whatever the surface inclination, as observed on rose petals.¹⁰ Indeed, for applications in water-harvesting systems, the best is to have the highest apparent contact angle while being completely sticky.

Table 2. Roughness (R_a and R_q) and Wettability Data for the PEDOP Polymers

polymer	deposition charge [mC cm^{-2}]	R_a [nm]	R_q [nm]	θ_w [deg]
PEDOP- <i>br</i> -C3	12.5	28	34	83
	25	20	25	89
	50	25	31	73
	100	136	175	79
	200	122	171	72
PEDOP- <i>br</i> -C5	400	154	218	72
	12.5	34	52	68
	25	25	32	64
	50	24	29	82
	100	110	140	74
PEDOP- <i>br</i> -C7	200	140	174	78
	400	250	312	68
	12.5	30	37	85
	25	95	123	63
	50	169	221	85
PEDOP- <i>br</i> -C11	100	200	257	45
	200	210	274	73
	400	402	595	68
	12.5	84	105	92
	25	61	79	97
PEDOP- <i>br</i> -C15	50	148	197	92
	100	155	203	96
	200	169	219	98
	400	620	838	79
	12.5	46	61	92
PEDOP- <i>br</i> -C18	25	62	78	88
	50	67	78	97
	100	55	65	98
	200	133	171	117
	400	165	208	132

In the case of ProDOP derivatives, crystal-like structures are obtained with ProDOP-*br*- C_{15} (Figure 6). Interestingly, the crystal-like structures look similar to the structures observed on lotus leaves.⁶ This is not surprising because the structures are in part composed of hydrocarbon waxes, which are composed of esters with very long alkyl chains. Using ProDOP-*br*- C_{18} , both large wrinkles and spherical nanoparticles are observed leading also to a high increase in θ_w up to 128° for $Q_s = 400 \text{ mC cm}^{-2}$ (Table 3).

3. CONCLUSIONS

Here, we chose to investigate the electrodeposition of PEDOP and PProDOP films with branched alkyl chains [from very short (C_3) to hyperbranched (C_{18})] grafted on the 3,4-alkylenedioxy bridge with the aim to favor the formation of nanofibers with parahydrophobic properties. It was easier to obtain insoluble polymer films with PEDOP polymers, whereas the polymer insolubility increased with the branched alkyl chain length. The formation of nanoparticles was more favored with the PEDOP polymers, whereas with the ProDOP polymers, it was possible to obtain nanofibers, resembling



Figure 7. Picture of a water droplet on a surface inclined to 90° obtained with EDOP-*br*-C₁₈ and with a deposition charge of 400 mC cm⁻². The droplet has a volume of 6 μL.

Table 3. Roughness (R_a and R_q) and Wettability Data for the PProDOP Polymers

polymer	deposition charge [mC cm ⁻²]	R_a [nm]	R_q [nm]	θ_w [deg]
PProDOP- <i>br</i> -C ₁₅	12.5	58	75	95
	25	48	58	99
	50	44	56	88
	100	132	167	100
	200	152	204	109
	400	395	612	105
PProDOP- <i>br</i> -C ₁₈	12.5	52	73	97
	25	66	76	98
	50	52	61	98
	100	92	121	104
	200	160	210	119
	400	374	494	128

wax nanoclusters observed on lotus leaves. Moreover, with both these PEDOP and PProDOP polymers, it was possible to reach parahydrophobic properties with extremely high water adhesion. These surface properties are extremely interesting and could be applied in the future for water harvesting systems, for example.

4. EXPERIMENTAL SECTION

4.1. Synthesis Way for the Monomers. As shown in Scheme 1, the monomers were synthesized in nine steps by adapting a procedure reported in the literature.³⁸ The key molecules were ProDOP-OH and EDOP-OH obtained by reaction with epibromohydrin, followed by nitrogen deprotection, saponification, and decarboxylation. Then, branched alkyl chains purchased from Sigma-Aldrich or TCI were grafted by simple esterification. More precisely, an absolute dichloromethane solution was prepared containing 1.2 equiv of alkanolic acid, 1.2 equiv of *N*-(3-dimethylaminopropyl)-*N*-ethylcarbodiimide hydrochloride, and *N,N*-dimethylaminopyridine as the catalyst. The solution was stirred for 30 min, and

an acetonitrile solution with 1 equiv of ProDOP-OH or EDOP-OH was added and the mixture was stirred for 1 day. Then, crude products were purified by column chromatography using tetrahydrofuran/petroleum ether at a ratio of 60:40 as the eluent. Triethylamine (10%) was added in silica gel to protect the very sensitive products.

The NMR spectra are given in the Supporting Information.

4.1.1. EDOP-*br*-C₃: (3,6-Dihydro-2H-[1,4]dioxino[2,3-*c*]pyrrol-2-yl)methyl Isobutyrate. Yield 87%; δ_H (200 MHz, CDCl₃): 7.11 (s, 1H), 6.20 (m, 2H), 4.32 (m, 3H), 4.21 (m, 1H), 4.03 (m, 1H), 2.61 (m, 1H), 1.18 (d, $J = 7.0$ Hz, 6H); δ_C (100 MHz, CDCl₃): 176.77, 132.18, 132.01, 98.66, 98.46, 72.25, 66.65, 62.46, 33.85, 30.30, 18.92; MS (ESI LC/MS): 226.00.

4.1.2. EDOP-*br*-C₅: (3,6-Dihydro-2H-[1,4]dioxino[2,3-*c*]pyrrol-2-yl)methyl 2-Ethylbutanoate. Yield 54%; δ_H (200 MHz, CDCl₃): 7.09 (s, 1H), 6.20 (m, 2H), 4.34 (m, 3H), 4.22 (m, 1H), 4.03 (m, 1H), 2.27 (m, 1H), 1.61 (m, 4H), 0.90 (t, $J = 7.4$ Hz, 6H); δ_C (100 MHz, CDCl₃): 175.87, 132.21, 132.01, 98.67, 98.44, 72.27, 66.70, 62.16, 48.71, 30.30, 24.94, 11.77; MS (ESI LC/MS): 254.00.

4.1.3. EDOP-*br*-C₇: (3,6-Dihydro-2H-[1,4]dioxino[2,3-*c*]pyrrol-2-yl)methyl 2-Propylpentanoate. Yield 93%; δ_H (200 MHz, CDCl₃): 7.17 (s, 1H), 6.20 (m, 2H), 4.33 (m, 3H), 4.20 (m, 1H), 4.02 (m, 1H), 2.46 (m, 1H), 1.60 (m, 4H), 1.30 (m, 4H), 0.89 (t, $J = 7.1$ Hz, 6H); δ_C (100 MHz, CDCl₃): 176.20, 132.15, 131.97, 98.64, 98.42, 72.22, 66.68, 62.15, 45.13, 34.51, 30.29, 26.88, 20.58, 13.96; MS (ESI LC/MS): 282.07.

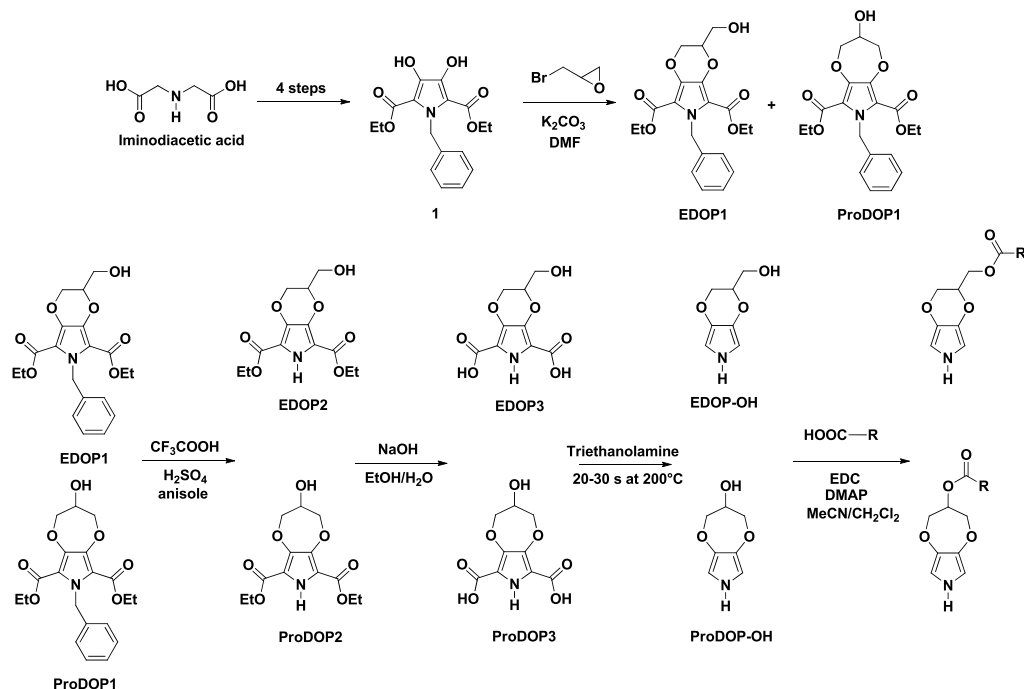
4.1.4. EDOP-*br*-C₁₁: (3,6-Dihydro-2H-[1,4]dioxino[2,3-*c*]pyrrol-2-yl)methyl 2-Butyloctanoate. Yield 82%; δ_H (200 MHz, CDCl₃): 7.10 (s, 1H), 6.20 (m, 2H), 4.33 (m, 3H), 4.22 (m, 1H), 4.02 (m, 1H), 2.42 (m, 1H), 1.60 (m, 4H), 1.25 (m, 12H), 0.87 (m, 6H); δ_C (100 MHz, CDCl₃): 176.23, 132.19, 132.01, 98.64, 98.42, 72.24, 66.70, 62.16, 45.58, 32.41, 32.38, 32.10, 32.07, 31.64, 30.30, 29.57, 29.19, 27.36, 22.57, 14.04, 13.91; MS (ESI LC/MS): 338.07.

4.1.5. EDOP-*br*-C₁₅: (3,6-Dihydro-2H-[1,4]dioxino[2,3-*c*]pyrrol-2-yl)methyl 2-Hexyldecanoate. Yield 66%; δ_H (200 MHz, CDCl₃): 7.12 (s, 1H), 6.20 (m, 2H), 4.33 (m, 3H), 4.20 (m, 1H), 4.02 (m, 1H), 2.40 (m, 1H), 1.60 (m, 4H), 1.25 (m, 20H), 0.87 (m, 6H); δ_C (100 MHz, CDCl₃): 176.23, 132.20, 132.01, 98.64, 98.42, 72.24, 66.71, 62.17, 45.61, 32.41, 32.38, 31.83, 31.64, 30.30, 29.54, 29.41, 29.23, 29.19, 27.40, 27.36, 22.64, 22.57, 14.08, 14.04; MS (ESI LC/MS): 394.20.

4.1.6. EDOP-*br*-C₁₈: (3,6-Dihydro-2H-[1,4]dioxino[2,3-*c*]pyrrol-2-yl)methyl 2-(4,4-Dimethylpentan-2-yl)-6,8,8-trimethylnonanoate. Yield 61%; δ_H (200 MHz, CDCl₃): 7.16 (s, 1H), 6.19 (m, 2H), 4.32 (m, 3H), 4.22 (m, 1H), 4.02 (m, 1H), 2.22 (m, 1H), 1.25 (m, 4H), 1.00 (m, 6H), 0.87 (m, 24H); δ_C (100 MHz, CDCl₃): 175.36, 175.33, 132.18, 131.98, 98.63, 98.39, 72.19, 66.77, 65.84, 62.13, 53.08, 52.96, 52.89, 52.82, 51.32, 51.26, 50.84, 48.37, 48.09, 46.17, 37.80, 37.71, 32.06, 32.02, 31.94, 31.87, 31.04, 31.01, 30.96, 30.29, 30.00, 29.96, 29.86, 29.68, 29.49, 29.44, 29.27, 29.18, 27.26, 27.16, 26.89, 26.03, 25.96, 22.79, 22.34, 20.22, 20.10, 19.94; MS (ESI LC/MS): 422.07.

4.1.7. ProDOP-*br*-C₃: 2,3,4,7-Tetrahydro-[1,4]dioxepino[2,3-*c*]pyrrol-3-yl Isobutyrate. Yield 74%; δ_H (200 MHz, CDCl₃): 7.19 (s, 1H), 6.31 (d, $J = 3.3$ Hz, 4H), 5.17 (m, 1H), 4.21 (dd, $J = 12.4$ Hz, $J = 4.9$ Hz, 2H), 4.08 (dd, $J = 12.4$ Hz, $J = 2.7$ Hz, 2H), 2.66 (m, 1H), 1.20 (d, $J = 7.0$ Hz, 6H); δ_C (100 MHz, CDCl₃): 176.53, 138.89, 103.07, 72.62, 72.46, 33.92, 30.30, 18.97; MS (ESI LC/MS): 225.93.

Scheme 1. Synthesis Way to the Monomers



4.1.8. *ProDOP-br-C₅*: 2,3,4,7-Tetrahydro-[1,4]dioxepino-[2,3-*c*]pyrrol-3-yl 2-Ethylbutanoate. Yield 48%; δ_{H} (200 MHz, CDCl_3): 7.19 (s, 1H), 6.31 (d, $J = 3.3$ Hz, 4H), 5.22 (m, 1H), 4.20 (dd, $J = 12.4$ Hz, $J = 4.9$ Hz, 2H), 4.08 (dd, $J = 12.4$ Hz, $J = 2.9$ Hz, 2H), 2.33 (m, 1H), 1.61 (m, 4H), 0.92 (t, $J = 7.4$ Hz, 6H); δ_{C} (100 MHz, CDCl_3): 175.57, 138.92, 103.06, 72.72, 72.35, 48.69, 30.30, 24.99, 11.74; MS (ESI LC/MS): 254.07.

4.1.9. *ProDOP-br-C₇*: 2,3,4,7-Tetrahydro-[1,4]dioxepino-[2,3-*c*]pyrrol-3-yl 2-Propylpentanoate. Yield 49%; δ_{H} (200 MHz, CDCl_3): 7.18 (s, 1H), 6.31 (d, $J = 3.3$ Hz, 4H), 5.21 (m, 1H), 4.19 (dd, $J = 12.4$ Hz, $J = 4.8$ Hz, 2H), 4.09 (dd, $J = 12.4$ Hz, $J = 3.1$ Hz, 2H), 2.48 (m, 1H), 1.60 (m, 4H), 1.29 (m, 4H), 0.90 (t, $J = 7.1$ Hz, 6H); δ_{C} (100 MHz, CDCl_3): 175.89, 138.91, 103.02, 72.70, 72.29, 45.16, 34.57, 30.30, 20.59, 14.00; MS (ESI LC/MS): 282.00.

4.1.10. *ProDOP-br-C₁₁*: 2,3,4,7-Tetrahydro-[1,4]dioxepino-[2,3-*c*]pyrrol-3-yl 2-Butyloctanoate. Yield 43%; δ_{H} (200 MHz, CDCl_3): 7.19 (s, 1H), 6.30 (d, $J = 3.3$ Hz, 4H), 5.21 (m, 1H), 4.17 (dd, $J = 12.4$ Hz, $J = 4.9$ Hz, 2H), 4.09 (dd, $J = 12.4$ Hz, $J = 3.3$ Hz, 2H), 2.41 (m, 1H), 1.63 (m, 4H), 1.26 (m, 12H), 0.89 (m, 6H); δ_{C} (100 MHz, CDCl_3): 175.88, 138.89, 103.00, 72.68, 72.26, 45.56, 32.41, 31.84, 31.66, 30.30, 29.53, 29.19, 27.32, 22.57, 14.05, 13.91; MS (ESI LC/MS): 338.07.

4.1.11. *ProDOP-br-C₁₅*: 2,3,4,7-Tetrahydro-[1,4]dioxepino-[2,3-*c*]pyrrol-3-yl 2-Hexyldecanoate. Yield 49%; δ_{H} (200 MHz, CDCl_3): 7.17 (s, 1H), 6.30 (d, $J = 3.3$ Hz, 4H), 5.21 (m, 1H), 4.18 (dd, $J = 12.4$ Hz, $J = 4.8$ Hz, 2H), 4.08 (dd, $J = 12.4$ Hz, $J = 3.3$ Hz, 2H), 2.43 (m, 1H), 1.59 (m, 4H), 1.25 (m, 20H), 0.87 (m, 6H); δ_{C} (100 MHz, CDCl_3): 175.88, 138.91, 103.07, 72.67, 72.26, 45.59, 32.41, 31.84, 31.66, 30.30, 29.53, 29.42, 29.22, 29.20, 27.37, 27.33, 14.09, 14.05; MS (ESI LC/MS): 394.20.

4.1.12. *ProDOP-br-C₁₈*: 2,3,4,7-Tetrahydro-[1,4]dioxepino-[2,3-*c*]pyrrol-3-yl 2-(4,4-Dimethylpentan-2-yl)-6,8,8-trimethylnonanoate. Yield 34%; δ_{H} (200 MHz, CDCl_3): 7.17 (s,

1H), 6.30 (d, $J = 3.2$ Hz, 4H), 5.17 (m, 1H), 4.15 (m, 4H), 2.23 (m, 1H), 1.25 (m, 4H), 1.00 (m, 6H), 0.87 (m, 24H); δ_{C} (100 MHz, CDCl_3): 175.00, 138.88, 102.99, 72.77, 72.74, 72.62, 72.58, 72.26, 53.03, 52.91, 52.86, 52.77, 51.29, 51.26, 50.86, 48.22, 48.04, 47.97, 37.70, 37.60, 32.11, 32.04, 32.00, 31.94, 31.05, 31.02, 30.97, 30.30, 30.00, 29.99, 29.92, 29.87, 29.68, 29.47, 29.44, 29.33, 29.17, 27.39, 27.21, 26.89, 26.24, 22.80, 22.34, 20.22, 20.10, 20.02; MS (ESI LC/MS): 422.20.

4.2. **Surface Preparation.** Electropolymerizations were realized with an Autolab potentiostat (Metrohm) and a three-electrode system. A glassy carbon rod was used as the counter electrode, and a SCE was used as the reference electrode. A platinum tip was first used as the working electrode to study the electropolymerization, whereas 2 cm² gold plates were used for surface characterization. Anhydrous acetonitrile (10 mL) was inserted inside the electrochemical cell and 0.1 M of tetrabutylammonium perchlorate (Bu_4NClO_4) and 0.01 M of monomer were added.

4.3. **Surface Characterization.** The surface properties were investigated using different equipment. The surface morphology was obtained by SEM using a 6700F microscope (JEOL). The arithmetic (R_a) and quadratic (R_q) surface roughness were determined with a WYKO NT1100 optical profiling system (Bruker). The measurements were realized with the working mode high-mag phase-shift interference, the objective 50 \times , and the field of view 0.5 \times .

For the surface-wetting properties, a DSA30 goniometer (Krüss) was used. Here, 2 μL of water droplets were slowly placed on the substrate. Thanks to a camera, the apparent contact angles are taken at the triple point. To characterize the adhesion behavior, 6 μL of water droplets was slowly placed on the substrate and the substrate was inclined until the droplet moves (tilted-drop method). The inclination inducing a deformation of the water droplet, the advanced and receding contact angle, and as a consequence, the hysteresis were taken but just before the droplet moves. If the droplet does not move

whatever the surface inclination, then the surface is called sticky.

■ ASSOCIATED CONTENT

■ Supporting Information

The Supporting Information is available free of charge on the ACS Publications website at DOI: 10.1021/acsomega.8b02026.

¹H and ¹³C NMR spectra (PDF)

■ AUTHOR INFORMATION

Corresponding Author

*E-mail: thierry.darmanin@unice.fr (T.D.).

ORCID

Frédéric Guittard: 0000-0001-9046-6725

Thierry Darmanin: 0000-0003-0150-7412

Notes

The authors declare no competing financial interest.

■ ACKNOWLEDGMENTS

The authors thank the Centre Commun de Microscopie Appliquée (CCMA) for the SEM images.

■ REFERENCES

- (1) Liu, K.; Yao, X.; Jiang, L. Recent Developments in Bio-Inspired Special Wettability. *Chem. Soc. Rev.* **2010**, *39*, 3240–3255.
- (2) Nosonovsky, M.; Bhushan, B. Superhydrophobic Surfaces and Emerging Applications: Non-Adhesion, Energy, Green Engineering. *Curr. Opin. Colloid Interface Sci.* **2009**, *14*, 270–280.
- (3) Tian, X.; Verho, T.; Ras, R. H. A. Moving Superhydrophobic Surfaces Toward Real-World Applications. *Science* **2016**, *352*, 142–143.
- (4) Liu, H.; Wang, Y.; Huang, J.; Chen, Z.; Chen, G.; Lai, Y. Bioinspired Surfaces with Superamphiphobic Properties: Concepts, Synthesis, and Applications. *Adv. Funct. Mater.* **2018**, *28*, 1707415.
- (5) Darmanin, T.; Guittard, F. Superhydrophobic and Superoleophobic Properties in Nature. *Mater. Today* **2015**, *18*, 273–285.
- (6) Koch, K.; Bhushan, B.; Barthlott, W. Multifunctional Surface Structures of Plants: An Inspiration for Biomimetics. *Prog. Mater. Sci.* **2009**, *54*, 137–178.
- (7) Sun, M.; Watson, G. S.; Zheng, Y.; Watson, J. A.; Liang, A. Wetting Properties on Nanostructured Surfaces of Cicada Wings. *J. Exp. Biol.* **2009**, *212*, 3148–3155.
- (8) Sun, Z.; Liao, T.; Sheng, L.; Kim, J. H.; Dou, S. X.; Bell, J. Fly Compound-Eye Inspired Inorganic Nanostructures with Extraordinary Visible-Light Responses. *Mater. Today Chem.* **2016**, *1–2*, 84–89.
- (9) Szczepanski, C. R.; Guittard, F.; Darmanin, T. Recent Advances in the Study and Design of Parahydrophobic Surfaces: From Natural Examples to Synthetic Approaches. *Adv. Colloid Interface Sci.* **2017**, *241*, 37–61.
- (10) Feng, L.; Zhang, Y.; Xi, J.; Zhu, Y.; Wang, N.; Xia, F.; Jiang, L. Petal Effect: A Superhydrophobic State with High Adhesive Force. *Langmuir* **2008**, *24*, 4114–4119.
- (11) Marmur, A. Hydro- Hygro- Oleo- Omni-Phobic? Terminology of Wettability Classification. *Soft Matter* **2012**, *8*, 6867–6870.
- (12) Bhushan, B.; Nosonovsky, M. The Rose Petal Effect and the Modes of Superhydrophobicity. *Philos. Trans. R. Soc., A* **2010**, *368*, 4713–4728.
- (13) Nuraje, N.; Khan, W. S.; Lei, Y.; Ceylan, M.; Asmatulu, R. Superhydrophobic Electrospun Nanofibers. *J. Mater. Chem. A* **2013**, *1*, 1929–1946.
- (14) Cengiz, U.; Avci, M.; Erbil, H. Y.; Sarac, A. S. Superhydrophobic Terpolymer Nanofibers Containing Perfluoroethyl Alkyl Methacrylate by Electrospinning. *Appl. Surf. Sci.* **2012**, *258*, 5815–5821.
- (15) Lai, Y.; Huang, J.; Cui, Z.; Ge, M.; Zhang, K.-Q.; Chen, Z.; Chi, L. Recent Advances in TiO₂-Based Nanostructured Surfaces with Controllable Wettability and Adhesion. *Small* **2016**, *12*, 2203–2224.
- (16) Lai, Y.; Pan, F.; Xu, C.; Fuchs, H.; Chi, L. In Situ Surface-Modification-Induced Superhydrophobic Patterns with Reversible Wettability and Adhesion. *Adv. Mater.* **2013**, *25*, 1682–1686.
- (17) Zhang, S.; Huang, J.; Tang, Y.; Li, S.; Ge, M.; Chen, Z.; Zhang, K.; Lai, Y. Understanding the Role of Dynamic Wettability for Condensate Microdrop Self-Propelling Based on Designed Superhydrophobic TiO₂ Nanostructures. *Small* **2017**, *13*, 1600687.
- (18) Darmanin, T.; Godeau, G.; Guittard, F. Superhydrophobic, Superoleophobic and Underwater Superoleophobic Conducting Polymer Films. *Surf. Innovations* **2018**, *6*, 181–204.
- (19) Tran, H. D.; Wang, Y.; D'Arcy, J. M.; Kaner, R. B. Toward an Understanding of the Formation of Conducting Polymer Nanofibers. *ACS Nano* **2008**, *2*, 1841–1848.
- (20) Park, H.; Lee, S. J.; Kim, S.; Ryu, H. W.; Lee, S. H.; Choi, H. H.; Cheong, I. W.; Kim, J.-H. Conducting Polymer Nanofiber Mats via Combination of Electrospinning and Oxidative Polymerization. *Polymer* **2013**, *54*, 4155–4160.
- (21) Zhu, Y.; Hu, D.; Wan, M. X.; Jiang, L.; Wei, Y. Conducting and Superhydrophobic Rambutan-like Hollow Spheres of Polyaniline. *Adv. Mater.* **2007**, *19*, 2092–2096.
- (22) Zhu, Y.; Li, J.; Wan, M.; Jiang, L. Superhydrophobic 3D Microstructures Assembled From 1D Nanofibers of Polyaniline. *Macromol. Rapid Commun.* **2008**, *29*, 239–243.
- (23) Huang, J. Syntheses and applications of conducting polymer polyaniline nanofiber. *Pure Appl. Chem.* **2006**, *78*, 15–27.
- (24) Fan, H.; Wang, H.; Guo, J.; Zhao, N.; Xu, J. Nanofibers-Based Nanoweb Promise Superhydrophobic Polyaniline: From Star-Shaped to Leaf-Shaped Structures. *J. Colloid Interface Sci.* **2013**, *409*, 255–258.
- (25) Zhao, Y.; Stejskal, J.; Wang, J. Towards Directional Assembly of Hierarchical Structures: Aniline Oligomers as the Model Precursors. *Nanoscale* **2013**, *5*, 2620–2626.
- (26) Lawal, A. T.; Wallace, G. G. Vapour Phase Polymerisation of Conducting and Non-Conducting Polymers: A Review. *Talanta* **2014**, *119*, 133–143.
- (27) Park, C.-S.; Kim, D.; Shin, B.; Kim, D.; Lee, H.-K.; Tae, H.-S. Conductive Polymer Synthesis with Single-Crystallinity via a Novel Plasma Polymerization Technique for Gas Sensor Applications. *Materials* **2016**, *9*, 812.
- (28) Roquet, S.; Leriche, P.; Perepichka, I.; Joussetme, B.; Levillain, E.; Frère, P.; Roncali, J. 3,4-Phenylenedioxythiophene (PheDOT): A Novel Platform for the Synthesis of Planar Substituted π -Donor Conjugated Systems. *J. Mater. Chem.* **2004**, *14*, 1396–1400.
- (29) Krompiec, M. P.; Baxter, S. N.; Klimareva, E. L.; Yufit, D. S.; Congrave, D. G.; Britten, T. K.; Perepichka, I. F. 3,4-Phenylenedioxythiophenes (PheDOTs) Functionalized with Electron-Withdrawing Groups and their Analogs for Organic Electronics. *J. Mater. Chem. C* **2018**, *6*, 3743–3756.
- (30) Qu, L.; Shi, G.; Chen, F.; Zhang, J. Electrochemical Growth of Polypyrrole Microcontainers. *Macromolecules* **2003**, *36*, 1063–1067.
- (31) Lin, H.-A.; Luo, S.-C.; Zhu, B.; Chen, C.; Yamashita, Y.; Yu, H.-h. Molecular or Nanoscale Structures? The Deciding Factor of Surface Properties on Functionalized Poly(3,4-ethylenedioxythiophene) Nanorod Arrays. *Adv. Funct. Mater.* **2013**, *23*, 3212–3219.
- (32) Diouf, A.; Darmanin, T.; Deng, S. Y.; Guittard, F. Superhydrophobic (Low Adhesion) and Parahydrophobic (High Adhesion) Surfaces with Micro/Nanostructures or Nanofilaments. *J. Colloid Interface Sci.* **2015**, *453*, 42–47.
- (33) Schottland, P.; Zong, K.; Gaupp, C. L.; Thompson, B. C.; Thomas, C. A.; Giurgiu, I.; Hickman, R.; Abboud, K. A.; Reynolds, J. R. Poly(3,4-alkylenedioxyppyrole)s: Highly Stable Electronically Conducting and Electrochromic Polymers. *Macromolecules* **2000**, *33*, 7051–7061.
- (34) Arroyave, F. A.; Reynolds, J. R. 3,4-Propylenedioxyppyrole-Based Conjugated Oligomers via Pd-Mediated Decarboxylative Cross Coupling. *Org. Lett.* **2010**, *12*, 1328–1331.

(35) Walczak, R. M.; Reynolds, J. R. Poly(3,4-alkylenedioxyppyroles): The PxDOPs as Versatile Yet Underutilized Electroactive and Conducting Polymers. *Adv. Mater.* **2006**, *18*, 1121–1131.

(36) Diouf, D.; Diouf, A.; Mortier, C.; Darmanin, T.; Dieng, S. Y.; Guittard, F. Poly(3,4-propylenedioxyppyrole) Nanofibers with Branched Alkyl Chains by Electropolymerization to Obtain Sticky Surfaces with High Contact Angles. *ChemistrySelect* **2017**, *2*, 9490–9494.

(37) Mortier, C.; Darmanin, T.; Guittard, F. Major Influence of the Hydrophobic Chain Length in the Formation of Poly(3,4-propylenedioxyppyrole) (PProDOP) Nanofibers with Special Wetting Properties. *Mater Today Chem.* **2018**, *7*, 65–75.

(38) Mortier, C.; Darmanin, T.; Guittard, F. Direct Electrodeposition of Superhydrophobic and Highly Oleophobic Poly(3,4-ethylenedioxyppyrole) (PEDOP) and Poly(3,4-propylenedioxyppyrole) (PProDOP) Nanofibers. *ChemNanoMat* **2017**, *3*, 885–894.

(39) Dai, X.; Sun, N.; Nielsen, S. O.; Stogin, B. B.; Wang, J.; Yang, S.; Wong, T.-S. Hydrophilic Directional Slippery Rough Surfaces for Water Harvesting. *Sci. Adv.* **2018**, *4*, No. eaaq0919.

(40) Poverenov, E.; Li, M.; Bitler, A.; Bendikov, M. Major Effect of Electropolymerization Solvent on Morphology and Electrochromic Properties of PEDOT Films. *Chem. Mater.* **2010**, *22*, 4019–4025.